

# Chemistry in oxygen-rich circumstellar envelopes

K. Willacy and T.J. Millar

Department of Physics, UMIST, PO Box 88, Manchester, UK

Received 9 December 1996 / Accepted 27 January 1997

**Abstract.** We have considered the chemistry occurring in the circumstellar envelope surrounding an oxygen-rich AGB star and have specifically modelled 4 sources; R Dor, TX Cam, OH231.8+4.2 and IK Tau. Methane has been assumed to be a parent molecule and the resulting carbon chemistry is investigated. We find that carbon chain molecules up to  $C_2H_4$  can be abundant as can  $CH_3CN$  and  $CH_3OH$ . Our model extends previous work by including the chemistry of silicon, chlorine and phosphorus. The presence of  $CH_4$  as a parent and hence its daughter species  $CH_3$  and  $CH_3^+$  leads to other carbon-bearing species such as  $H_2CS$ ,  $SiCH_2$ ,  $H_2CN$  and  $CCl$ .

Sulphur is an important source of electrons in some regions of the envelope. Its main effect is on the abundance of  $CH_3^+$  and molecules formed from this radical e.g.  $CH_3OH$ .

Where possible we have compared our results to observations and in general there is good agreement. A notable exception is the case of OCS in OH231.8+4.2 whose calculated abundance is roughly  $10^4$  times lower than observed.

**Key words:** stars: abundances – stars: circumstellar matter – stars: late type

---

## 1. Introduction

LTE calculations of the chemistry of the circumstellar envelopes (CSEs) surrounding oxygen-rich late type stars show the carbon to be tied up in CO with the excess oxygen forming other molecules such as  $H_2O$  (Tsuji 1973). So the first observations of other carbon-bearing molecules in such sources were somewhat unexpected. Several carbon-bearing molecules have now been observed: HCN,  $HCO^+$ , CS, OCS, HNC, CN (Deguchi & Goldsmith 1985; Jewell, Snyder & Schenewerk 1986; Omont et al. 1986; Lindqvist et al. 1988, 1992; Nercessian et al. 1989; Olofsson et al. 1991; Bujarrabal, Fuente & Omont 1994). It has been suggested that such molecules arise from the breakdown of  $CH_4$  which is assumed to be a parent molecule, formed in the inner envelope, possibly by grain surface reactions (Nejad & Millar 1988) or by UV/shock chemistry (Nercessian et al 1989). The

presence of methane has also been used by Millar & Olofsson (1993) to account for observations of  $H_2CO$  in OH231.8+4.2 (Lindqvist et al. 1992). Charnley, Tielens & Kress (1995) have predicted that the inclusion of  $CH_4$  in the chemistry will result in high abundances of  $CH_3OH$ ,  $C_2H$  and  $C_2$  with  $C_2H_4$ ,  $C_2H_2$  and  $CH_3CN$  also being present.

In this paper we extend the previous models to include the chemistry of silicon, phosphorus and chlorine. We investigate the effects of  $CH_4$  on the carbon chemistry. We model four sources in detail and compare our results to the available observations.

## 2. The model

The model is based on that of Nejad & Millar (1988) and involves 200 species linked by 1909 reactions. The reaction rates are taken from the UMIST database RATE95 (Millar, Farquhar & Willacy 1996) with additional phosphorus reactions from Charnley & Millar (1994). Cosmic ray ionization processes are included. For those neutral species without a tabulated photodestruction rate, a rate of  $1.1 \times 10^{-9} \exp(-2A_V)$  is used. Because of its effective self-shielding,  $H_2$  is assumed to remain unaffected by photodissociation over the region of the envelope which we consider. The photodissociation of CO is treated using the approximation of Morris & Jura (1983). The initial abundances of the parent species are given in Table 1.

The CSE is assumed to be spherically symmetric with an expansion velocity,  $v_e$ , and a constant mass loss rate,  $\dot{M}$ . We have modelled 4 sources, 3 of which are well observed, with different values of  $\dot{M}$ . The physical parameters are given in Table 2. There is some debate in the literature as to the exact values of these parameters. We have used the values given in Bujarrabal et al (1994) for IK Tau and TX Cam and in Omont et al (1993) for OH231.8+4.2. In each case the chemical abundances are calculated as a function of radius, beginning at an inner radius,  $r_0$ , of  $2 \times 10^{15}$  cm and continuing outwards until all the molecules have been destroyed by photodissociation. The radial number density of  $H_2$  is given by

$$n(r) = \dot{M} / (4\pi r^2 v_e m) \quad (1)$$

where  $m$  is the mass of molecular hydrogen.

**Table 1.** The fractional abundances (relative to H<sub>2</sub>) taken for the parent species

Parent species	Fractional abundance	Parent species	Fractional abundance
H <sub>2</sub> O	3.0 (-4)	CH <sub>4</sub>	3.0 (-5)
SiS	3.5 (-6)	H <sub>2</sub> S	1.27 (-5)
NH <sub>3</sub>	1.0 (-5)	CO	4.0 (-4)
N <sub>2</sub>	5.0 (-5)	SiO	3.15 (-5)
He	0.1	PH <sub>3</sub>	3.0 (-8)
HCl	4.4 (-7)		

**Table 2.** The physical parameters used to model each source. The values are taken from (1) Omont et al 1993; (2) Bujarrabal et al (1994); (3) Lindqvist et al (1992)

Source	$\dot{M}$ ( $M_{\odot} \text{ yr}^{-1}$ )	$v_e$ ( $\text{kms}^{-1}$ )	D (pc)
OH 231.8+4.2 <sup>1</sup>	1.0 (-4)	30.0	1300
IK Tau <sup>2</sup>	4.5 (-6)	20.0	270
TX Cam <sup>2</sup>	3.0 (-6)	18.0	350
R Dor <sup>3</sup>	1.0 (-7)	6.0	230

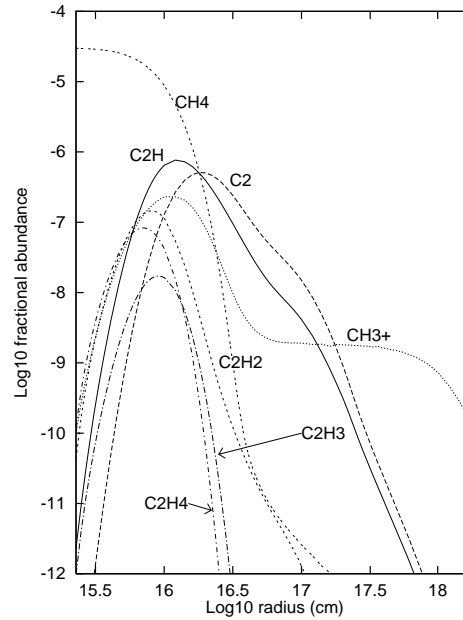
The temperature is described by a power law

$$T(r) = T(r_0) \left( \frac{r_0}{r} \right)^{0.6} \quad (2)$$

where  $T(r_0)$  is taken to be 100 K for those sources with  $\dot{M} > 5 \times 10^{-6} M_{\odot}$  and 300 K otherwise (Millar & Olofsson 1993). This is an approximation to the temperature profile in the envelope. In the outermost parts the temperature will be higher than given by this equation since the influence of photoelectric heating by the external interstellar radiation field becomes important. However at this distance from the star the density is low and the chemistry is driven by the UV photons rather than by collisions. In addition the major chemical reactions have rates which are either independent of temperature or which depend on  $T^{-0.5}$  so that the rate is only weakly dependent on the radius. Hence in the region of the CSE that we are considering the chemistry is relatively temperature independent and the exact nature of the power law is unimportant.

### 3. The chemistry of the circumstellar envelope

The envelope chemistry can roughly be divided into 3 zones: an inner region where the parent molecules begin to break down, a peak region where the daughter molecules reach their peak abundances and an outer region where the photons finally photodissociate all the molecules. The abundance distributions are illustrated by the case of TX Cam. The chemistry in the three zones does not vary with mass loss rate. Therefore the discussion which follows is valid for all 4 models. What does vary with  $\dot{M}$  are the radii at which the various regions arise, with  $r$  increasing with  $\dot{M}$ .

**Fig. 1.** The fractional abundance of the carbon-chain molecules as a function of radius for TX Cam.

#### 3.1. Initiating the chemistry

At very small radii, ions as well as photons are important in driving the chemistry by breaking down the parent molecules. Cosmic rays produce H<sub>3</sub><sup>+</sup> by



Once this is present other ions can be formed e.g.



The role played by these ions in the chemistry is discussed below.

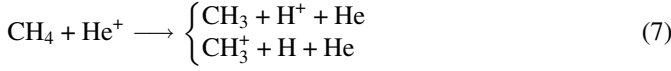
#### 3.2. Carbon chain chemistry

Carbon is contained in two parent molecules, CO and CH<sub>4</sub>. Previous work (Nejad & Millar 1988) has shown that carbon is not released from CO in sufficient quantities to drive the carbon chemistry. So the presence of carbon chains in our model is due to the breakdown of CH<sub>4</sub>.

The fractional abundance of the carbon chain molecules as a function of radius is shown in Fig. 1. It can be seen that, except in the outer region, the distributions of the chain molecules follow that of CH<sub>3</sub><sup>+</sup>.

## 3.2.1. The inner region

The main destruction processes for CH<sub>4</sub> are photodissociation to CH<sub>2</sub> and reaction with H<sub>3</sub><sup>+</sup> forming CH<sub>5</sub><sup>+</sup>. Some CH<sub>4</sub> is also broken down into CH<sub>3</sub> and CH<sub>3</sub><sup>+</sup> by



and

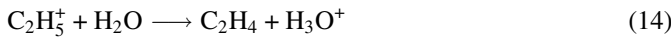
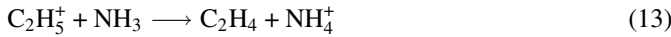


The reaction of CH<sub>3</sub><sup>+</sup> with H<sub>2</sub> is much slower than for the other CH<sub>n</sub><sup>+</sup> species. Hence it has the opportunity to react with other molecules, initiating a rich chemistry.

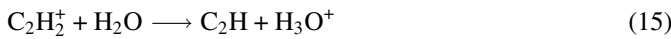
In the inner zone the chemistry is driven by



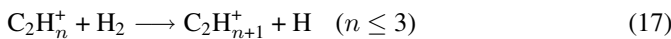
These ions can then react with the most abundant neutral species, H<sub>2</sub>O, NH<sub>3</sub> or H<sub>2</sub>:



and

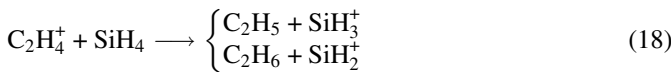


Only those C<sub>2</sub>H<sub>n</sub> molecules with  $n \leq 4$  are abundant. In these cases the ion chains build up by



and the ions are converted into neutrals by proton transfer reaction with the parent molecules NH<sub>3</sub> and H<sub>2</sub>O.

The addition of H<sub>2</sub> to form C<sub>2</sub>H<sub>n</sub><sup>+</sup> with  $n > 4$  does not occur and C<sub>2</sub>H<sub>5</sub> and C<sub>2</sub>H<sub>6</sub> are formed by



Since SiH<sub>4</sub> has a very low abundance, these processes are inefficient and C<sub>2</sub>H<sub>5</sub> and C<sub>2</sub>H<sub>6</sub> are not present in the gas to any significant degree.

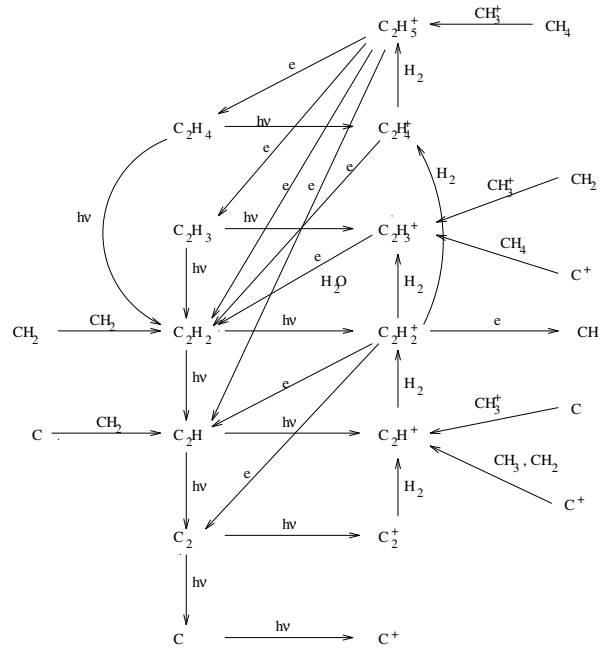
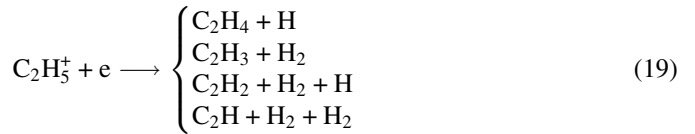


**Fig. 2.** The carbon chain chemistry in the peak region. Here destruction by photons rather than by reaction with ions is the major means of removing the neutral species.

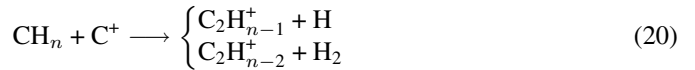
## 3.2.2. The peak region

As the radius increases so does the importance of the photodestruction of the carbon chain neutrals, converting them into ions (see Fig. 2). The ions are now mainly destroyed by dissociative recombination with electrons e.g.



although reaction with H<sub>2</sub>O is still important in the formation of C<sub>2</sub>H<sub>4</sub> (from C<sub>2</sub>H<sub>5</sub><sup>+</sup>) and C<sub>2</sub>H<sub>2</sub> (from C<sub>2</sub>H<sub>3</sub><sup>+</sup>).

There are still several routes into the chemistry from the reactions



for  $n = 0, 1, \dots, 4$  and from CH<sub>3</sub><sup>+</sup> reacting with CH<sub>4</sub> and CH<sub>2</sub> to form C<sub>2</sub>H<sub>5</sub><sup>+</sup> and C<sub>2</sub>H<sub>3</sub><sup>+</sup> respectively.

## 3.2.3. The outer region

The chemistry in this region is similar to that at the smaller radii except that photoreactions are now of increased importance. Molecules are destroyed and most of the carbon is in C<sup>+</sup>. One change in the chemistry is that the reaction of C<sub>2</sub>H with Si<sup>+</sup> followed by dissociative recombination



is now a major source of  $C_2$ , producing more of this molecule than the direct conversion from  $C_2H$  by photoprocessing.

### 3.3. Other carbon-bearing molecules

At small radii the parent molecules are generally destroyed by reactions with ions rather than by interactions with photons. One of these ions is  $HCO^+$  which is formed by

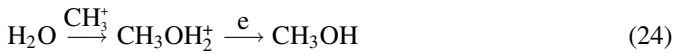


The first carbon-oxygen bearing molecule to be formed is  $CO_2$  from the reaction of  $OH$  and  $CO$



Cosmic rays can also destroy  $CO$  producing  $CO^+$ .

Methanol is formed entirely from



once again demonstrating the importance of the presence of  $CH_3^+$  for the carbon chemistry. This ion also aids the formation of  $CH_2CO$ :



$H_2CO$  on the other hand is formed from neutral-neutral reactions



Fig. 3 shows the abundances of various carbon-bearing species.

### 3.4. Nitrogen chemistry

#### 3.4.1. The inner region

At this low value of the radius photodestruction of the strongly bound parent  $N_2$  is not important. Instead it is destroyed by:

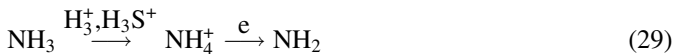


$N^+$  reacts with  $H_2$  to form the nitrogen hydride ions



while the nitrogen atoms react with  $OH$  forming  $NO$ .

The first daughter species to appear is  $NH_2$ . It is formed from the breakdown of  $NH_3$  which occurs mainly by reaction with ions:



There is also a small ( $\sim 10\%$ ) contribution from the direct photodissociation of  $NH_3$

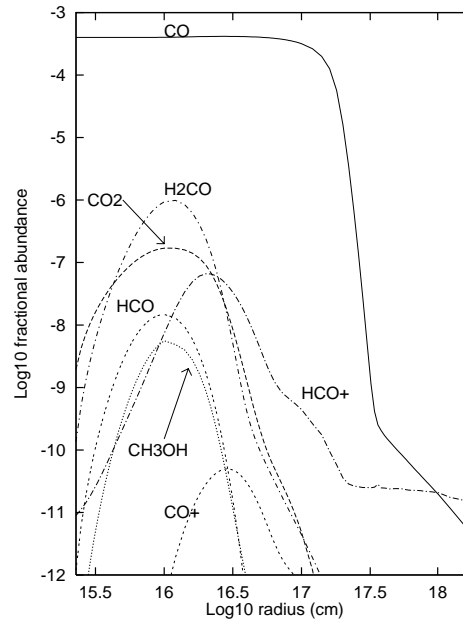
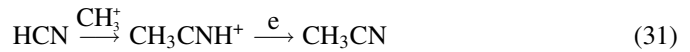


**Fig. 3.** The radial distribution of carbon- and oxygen-bearing molecules in TX Cam.

The formation of  $HCN$  and related compounds depends on the reactions of  $NH_3$  as shown in Fig. 5. The  $C^+$  ion is important in destroying  $NH_3$  and hence in the formation of  $HNC$  and  $CN$ . At all points in the envelope  $CH_3CN$  is formed by



and destroyed by photons.

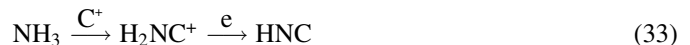
#### 3.4.2. The peak region

Moving out from the star the gas density is reduced and the interstellar radiation field is able to penetrate leading to an increased importance of photoreactions. The main destruction process for  $N_2$  is now photodissociation resulting in two nitrogen atoms. A small amount of  $N_2$  is still converted into  $N^+$  by reaction with  $He^+$  and continues to contribute to the formation of  $NH_n^+$  (reaction 28). The formation route of  $HCN$  has however changed (Fig. 6).

$HCN$  and  $CN$  are now produced by neutral-neutral reactions, with  $HNC$  mainly formed by ion-molecule reactions.  $HCN$  is formed directly from the reaction of  $NO$  with  $CH$  or from



It is rapidly dissociated into  $CN$  and then into its constituent atoms.  $NO$ , the most abundant nitrogen-bearing molecule in this region, is also involved in the formation of  $CN$  by its reaction with carbon atoms. Another route to  $CN$  is via the reaction of carbon atoms with  $NH$ .  $HNC$  on the other hand is a result of either



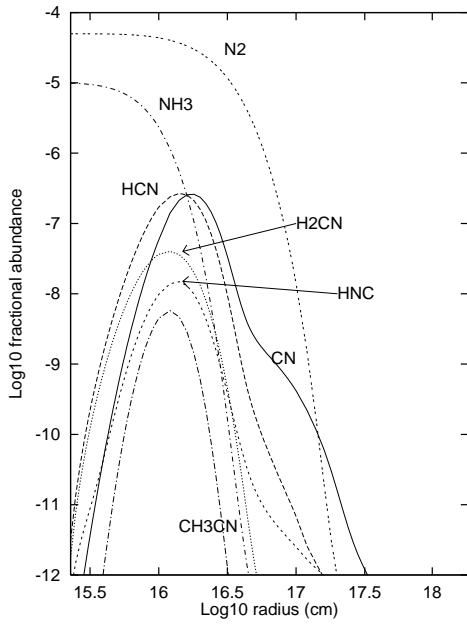


**Fig. 4.** The radial distributions of some nitrogen-bearing molecules in TX Cam.

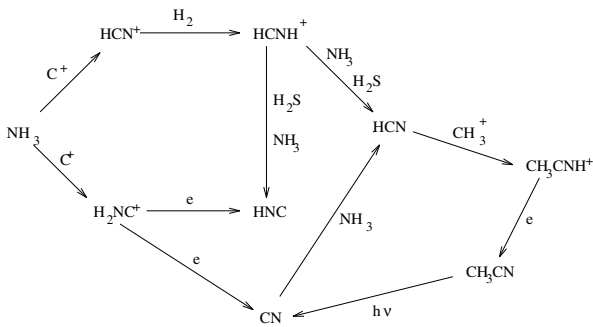
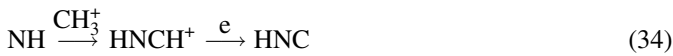


**Fig. 5.** The main reactions forming carbon-nitrogen compounds in the inner region.

or

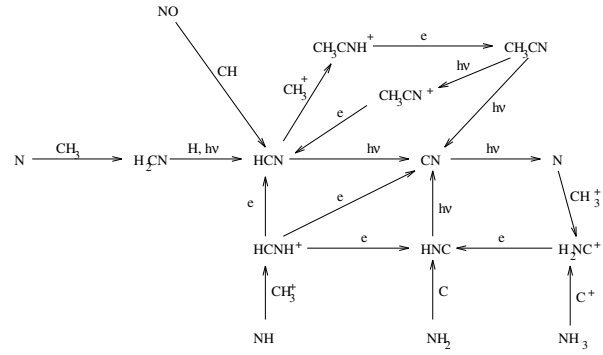


The recombination of  $\text{HCNH}^+$  with electrons can also result in HCN and CN but for these molecules the other formation routes mentioned above are more efficient. About 30% of the HNC is formed by the neutral-neutral reaction between carbon atoms and  $\text{NH}_2$ .

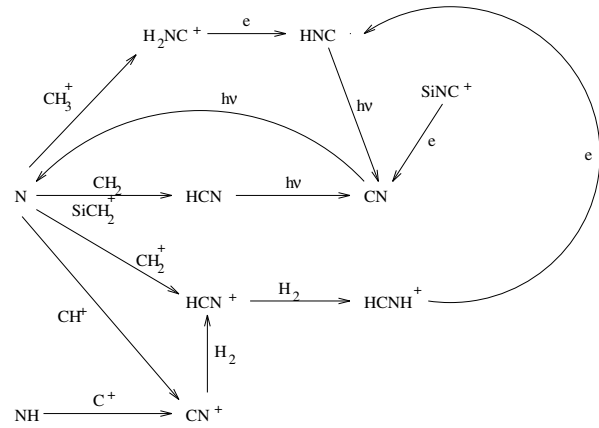
### 3.4.3. The outer region

Fig. 7 shows the nitrogen-carbon chemistry at large radii.

The abundance of ammonia is now too low to play a part in the chemistry but its daughter species N and NH are important. HCN is now produced by the reaction of nitrogen atoms with either  $\text{CH}_2$  or  $\text{SiCH}_2^+$ . The dominant route to HNC is through  $\text{H}_2\text{NC}^+$ , with only a small ( $\sim 6\%$ ) contribution from  $\text{HCNH}^+$ .



**Fig. 6.** The nitrogen chemistry in the peak region. The reactions of nitrogen atoms are now more important than those of  $\text{NH}_3$  in forming nitrogen-carbon compounds.



**Fig. 7.** The nitrogen-carbon chemistry in the outer region. At this point there is net destruction of the molecules due to the photon field.

Overall the molecules are destroyed by the photon field and abundances are very low.

### 3.5. Silicon chemistry

The parent molecules for silicon are SiS and SiO. The radial distributions of some important molecules are shown in Fig. 8.  $\text{SiO}_2$  is the most abundant of the silicon bearing molecules formed in our model which also predicts high abundances of  $\text{SiCH}_2$ ,  $\text{HCSi}$ ,  $\text{SiC}$  and  $\text{SiN}$ .

#### 3.5.1. Initiating the chemistry

The parent molecules are not destroyed by photons at small radii. Instead reactions with ions are important:



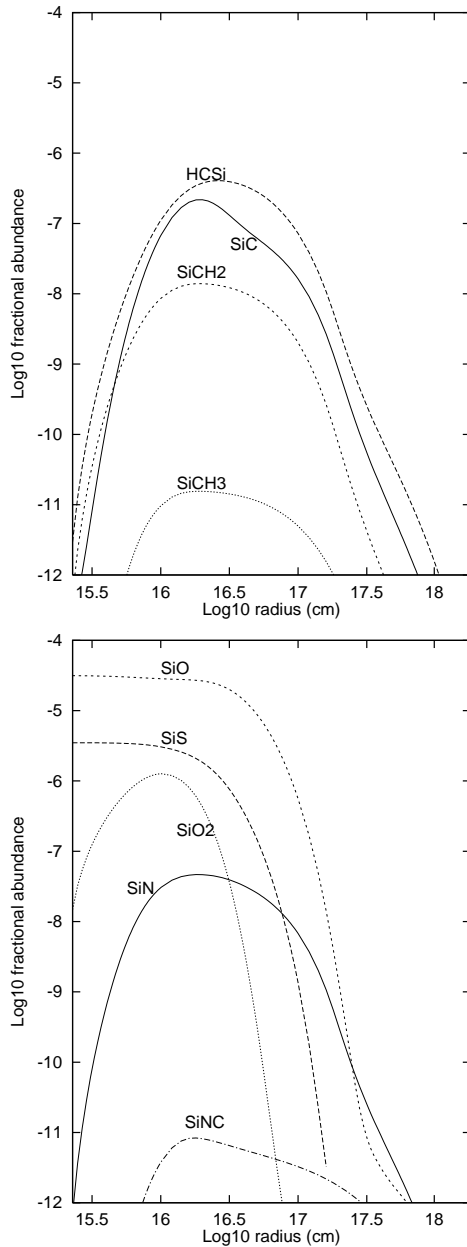


**Fig. 8.** The radial distributions of some important silicon-bearing molecules in TX Cam.

Initially silicon ions are formed by the reactions of SiS or SiO with  $\text{He}^+$  and  $\text{C}^+$  but as the radius increases photodissociation becomes more important:



Once the silicon atoms and ions are present other silicon-bearing molecules can be formed.

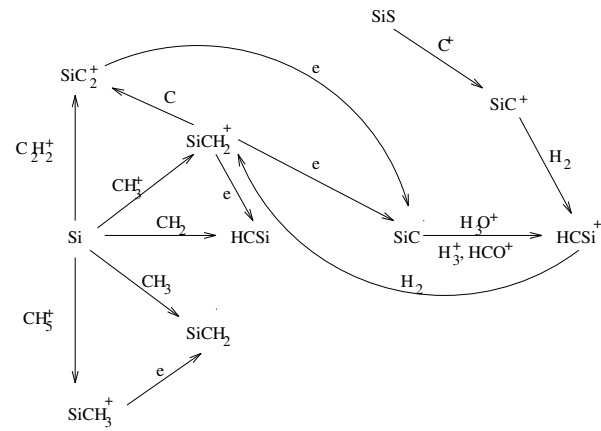


**Fig. 9.** The silicon and carbon chemistry in the inner region.

### 3.5.2. Silicon-carbon compounds

The main processes involving silicon and carbon molecules in the inner region are shown in Fig. 9.

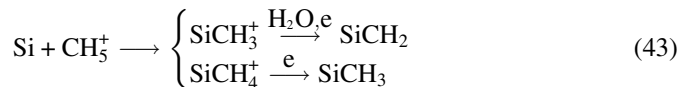
HCSi and SiC are the silicon-carbon bearing molecules with the highest abundances. Both form from the dissociative recombination of  $\text{SiCH}_2^+$  which can only be produced if  $\text{CH}_4$  is present as a parent:



HCSi is also formed directly from



Larger silicon-carbon molecules can also form in appreciable quantities e.g.



As the radius increases, the chemistry is driven more by reactions of  $\text{Si}^+$  than by reactions of Si.  $\text{Si}^+$  can react with  $\text{CH}_n$ :



(which is now the main route to  $\text{SiC}^+$  with virtually no contribution from the  $\text{SiS} + \text{C}^+$  reaction which dominates at small radii),



In the outer layers of the CSE, SiC is mainly formed by the  $\text{SiC}_2^+$  route (see Fig. 9). Its conversion into  $\text{SiC}^+$  is achieved by reaction with  $\text{C}^+$  which is now the dominant ion.

### 3.5.3. Other silicon compounds

$\text{Si}^+$  reacts with  $\text{NH}_3$  to form  $\text{SiNH}_3^+$ . From this, dissociative recombination produces  $\text{SiN}$  and  $\text{HNSi}$  while reaction with carbon atoms results in  $\text{SiNCH}$ . At small radii  $\text{HNSi}$  is mainly destroyed by



but as the radius increases and the abundance of  $\text{C}^+$  rises



becomes more important.

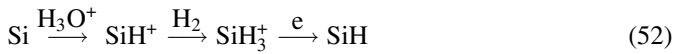
$\text{SiN}$  is destroyed by reaction with oxygen atoms in the peak region forming  $\text{SiO}$ . Again reaction with  $\text{C}^+$  becomes significant at larger radii producing  $\text{SiC}^+$  or  $\text{SiN}^+$ .

$\text{SiO}_2$  is formed at all radii by



and destroyed mainly by photodissociation.

Of the silicon hydrides only  $\text{SiH}$  is abundant. In the inner region it is formed by one of three routes:



or



As the radius increases reaction 53 becomes the only important route until the abundance of  $\text{SiCH}_2^+$  drops after which, in the outer region, reaction 51 is the major formation process. Destruction is by photodissociation into  $\text{Si}$  and  $\text{H}$ .

### 3.6. Sulphur chemistry

Several sulphur-bearing molecules have high fractional abundances as can be seen in Fig. 10. Initially sulphur is contained in  $\text{SiS}$  and  $\text{H}_2\text{S}$ . The first molecules to appear are  $\text{HS}$  and  $\text{CS}$ .  $\text{HS}$  arises from the breakdown of the parent molecules by reaction with ions e.g.



or by photodissociation



$\text{HS}$  is also a product of reaction 36.

Both  $\text{S}$  and  $\text{S}^+$  are unreactive with  $\text{H}_2$  but they can react with other molecules, e.g. with  $\text{OH}$  to form  $\text{SO}$ . However in this region the major route to  $\text{SO}$  is by the reaction of  $\text{HS}$  with oxygen atoms.

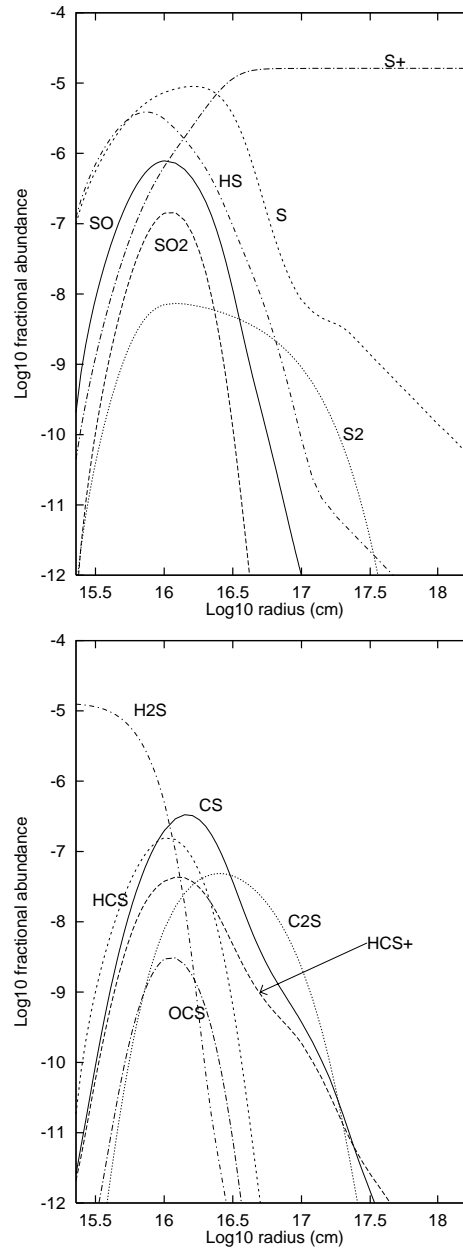


**Fig. 10.** The abundances of important sulphur-bearing molecules in the circumstellar envelope of TX Cam.

The carbon sulphides are formed by



and



while  $\text{HCS}$  arises either from the dissociative recombination of  $\text{HC}_2\text{S}^+$  or from the reaction of  $\text{S}$  with  $\text{CH}_2$ .

The main chemical pathways involving sulphur and oxygen are shown in Fig. 11.

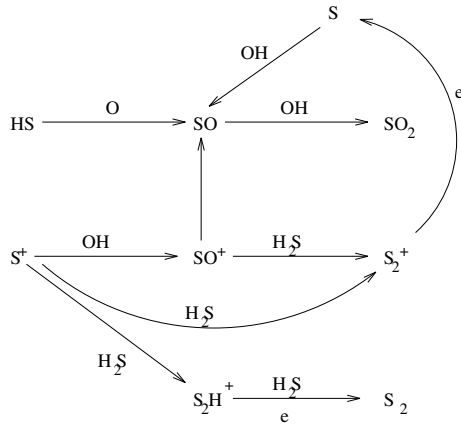
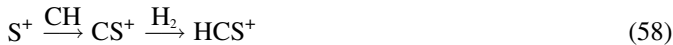


**Fig. 11.** The sulphur and oxygen chemistry in the inner region.

### 3.6.1. The peak region

As the abundance of sulphur atoms rises so does the importance of the  $S + OH$  route to  $SO$  and in this region of the CSE it is the main formation process of this molecule. In addition, there is now a sizeable contribution from the photodissociation of  $SO_2$ .  $SO$  is itself photodissociated into its constituent atoms, either directly or via  $SO^+$ .

$H_2S$  is now longer the most abundant sulphur species and its importance is diminished with the chemistry now being driven by  $S$ ,  $S^+$  and  $HS$  (see Fig. 11).  $HCS^+$  is formed by the two stage process



The recombination of  $HCS^+$  with electrons is still the most efficient way of forming  $CS$  but, in addition, the reactions of  $SO$  and  $HS$  with carbon atoms are now important.



### 3.6.2. Other sulphur-bearing molecules

$OCS$  has been observed in one source, OH231.8+4.2. It is produced by



with



also being an important mechanism. Where  $CH_3^+$  is not abundant  $OCS$  arises from the radiative association of  $CO$  and  $S$ .

At all radii  $NS$  can be produced by

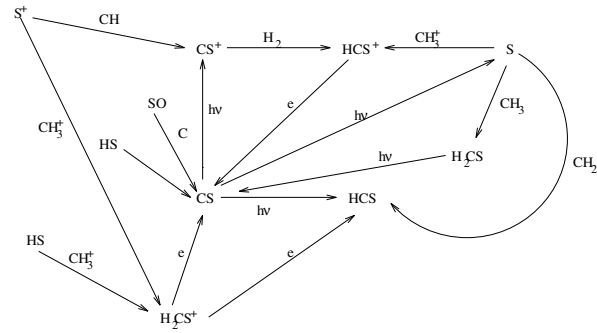


**Fig. 12.** The sulphur and carbon chemistry in the peak region.

At the abundance peak there is a second formation process



It is destroyed by oxygen atoms forming  $NO$ , with reactions with  $C^+$  (leading to  $NS^+$  and  $CS^+$ ) and photodissociation (into its constituent atoms) becoming more important as the radius increases.

$S_2$  is quite abundant in the outer layers of the CSE where it is produced by



Near the radius corresponding to its peak abundance it is partly destroyed by reaction with oxygen atoms forming  $SO$ . Moving further out photon reactions become the major source of destruction.

$H_2CS$  is another molecule whose distribution depends on the presence of  $CH_4$  as a parent molecule. Near its peak it is produced by



At very small or very large radii it arises from



It is destroyed by photoreactions producing  $CS$  and  $H_2$ .

### 3.6.3. The effect of the sulphur chemistry on other molecules

Sulphur can be an important source of electrons, thereby increasing the influence of ion-molecule reactions on the chemistry. We have run our models for two sources, R Dor and OH231.8+4.2 excluding sulphur. The effect of this on the abundance of the carbon-bearing molecules is shown in Table 3.

The removal of sulphur from the model causes an increase in the peak abundance of  $CH_3^+$  of about 60%. This causes a corresponding increase in the abundances of those carbon bearing molecules which depend on the presence of  $CH_3^+$  for their existence e.g.  $C_2H_4$ . The effect is most marked in the higher mass loss rate model.  $CH_3$  is not affected by the presence of sulphur and its abundance and that of molecules such as  $H_2CN$  remains



**Table 3.** The peak fractional abundances of selected molecules for the models of R Dor and OH231.8+4.2. Two values are given for each model, where the sulphur chemistry has been included or excluded.

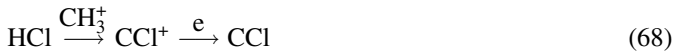
Species	R Dor		OH231.8+4.2	
	with S	without S	with S	without S
CH <sub>3</sub> <sup>+</sup>	3.1 (-7)	5.0 (-7)	8.2 (-8)	1.3 (-7)
CH <sub>3</sub>	2.2 (-6)	2.2 (-6)	2.0 (-6)	2.2 (-6)
C <sub>2</sub>	4.2 (-7)	5.9 (-7)	2.0 (-7)	2.8 (-7)
C <sub>2</sub> H	6.2 (-7)	8.2 (-7)	2.0 (-7)	3.0 (-7)
C <sub>2</sub> H <sub>2</sub>	1.0 (-7)	1.2 (-7)	3.2 (-8)	4.4 (-8)
C <sub>2</sub> H <sub>3</sub>	1.8 (-8)	2.3 (-8)	8.6 (-9)	1.1 (-8)
C <sub>2</sub> H <sub>4</sub>	3.8 (-8)	5.8 (-8)	3.5 (-8)	4.9 (-8)
CH <sub>3</sub> OH	1.2 (-8)	1.6 (-8)	3.5 (-8)	5.1 (-8)
H <sub>2</sub> CO	9.3 (-7)	9.5 (-7)	5.0 (-7)	5.1 (-7)
C <sub>2</sub> H <sup>+</sup>	1.1 (-11)	1.7 (-11)	3.6 (-12)	5.6 (-12)
C <sub>2</sub> H <sub>5</sub> <sup>+</sup>	4.0 (-9)	6.8 (-9)	1.4 (-9)	2.5 (-9)
H <sub>2</sub> CN	4.8 (-8)	5.0 (-8)	2.2 (-8)	2.3 (-8)
CH <sub>3</sub> CN	5.0 (-9)	8.3 (-9)	1.4 (-9)	2.4 (-9)
SiCH <sub>2</sub>	9.5 (-9)	8.8 (-9)	7.0 (-9)	6.4 (-9)
SiCH <sub>2</sub> <sup>+</sup>	9.9 (-9)	1.4 (-8)	4.1 (-9)	5.4 (-9)
HCSi <sup>+</sup>	1.4 (-11)	9.3 (-12)	5.2 (-12)	3.4 (-12)
CCl	9.8 (-9)	1.5 (-8)	4.2 (-9)	6.3 (-9)

the same. The smaller carbon chain molecules (C<sub>2</sub>H<sub>*n*</sub> where *n* = 0, 1, 2) are also relatively unaffected by the presence of sulphur. They have alternative formation processes which do not depend on CH<sub>3</sub><sup>+</sup> and these become more important in the presence of sulphur.

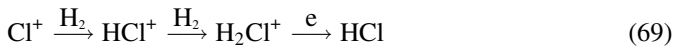
### 3.7. Chlorine chemistry

The formation of ClO is inhibited by the presence of high activation energy barriers and we have therefore assumed it is not present in the gas. Instead we have considered the parent molecule to be HCl.

The chlorine chemistry does not change much with radius and is shown in Fig. 13. The most abundant molecule formed in the CSE is CCl which arises from:



At low radii there is a route from HCl to Cl<sup>+</sup> by reaction with He<sup>+</sup> in addition to the photodestruction process shown in Fig. 13. At large radii HCl is still abundant. Its formation, by reactions of H<sub>2</sub> with chlorine-bearing ions:



and destruction (by photons) are almost in equilibrium. The abundance of HCl will fall off as the photon field destroys H<sub>2</sub>.

### 3.8. Phosphorus chemistry

The only phosphorus-bearing species with fractional abundances greater than 10<sup>-10</sup> are P, PH, PH<sub>2</sub>, PH<sub>3</sub> and PO. Their distributions are shown in Fig. 14. The chemistry is driven by

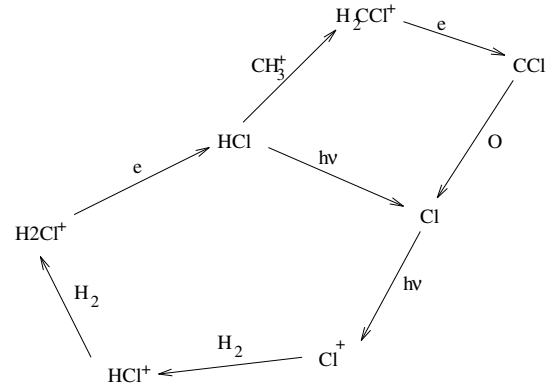


**Fig. 13.** The chlorine chemistry in a circumstellar envelope. The reactions do not vary with radius other than for the photoreactions to assume an increased importance as the radius increases.

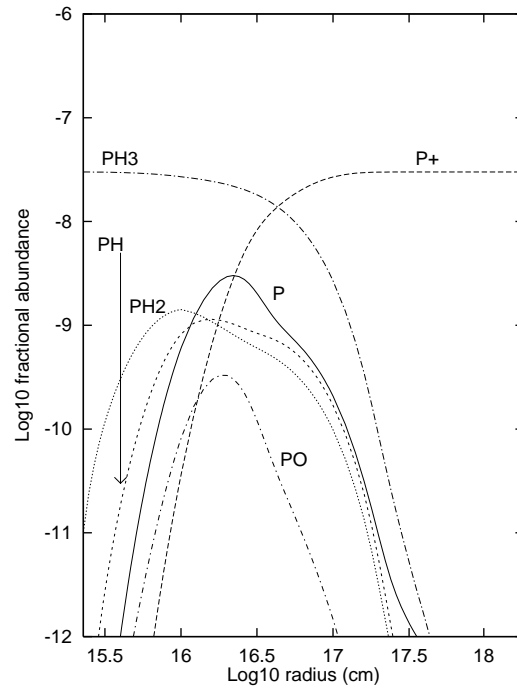


**Fig. 14.** The radial distribution of the phosphorus molecules in OH231.8+4.2

the destruction of the parent molecule, PH<sub>3</sub>, by reaction with ions:



with reaction 72 becoming more important as the radius increases. Photodissociation is not important even at large radii. The other hydride molecules are formed by recombination



**Table 4.** A comparison of the observed peak fractional abundances with those calculated in the model for OH231.8+4.2. The observations are taken from (1) Morris et al (1987); (2) Bujarrabal et al (1994); (3) Lindqvist et al (1992); (4) Charnley & Latter (1996). The observed values vary greatly. This is probably due to different assumptions as to the excitation temperature and the radial extent of the emission.

Species	Model	Observations			
		1	2	3	4
HCN	1.0 (-7)	3.9 (-7)	4.4 (-6)	3.0 (-7)	
HNC	1.8 (-8)	1.8 (-7)	7.9 (-7)		
CS	2.4 (-7)	2.8 (-7)	7.5 (-7)		
SiO	3.2 (-5)	7.8 (-8)	7.7 (-7)		
SO	1.0 (-6)	2.1 (-6)	4.0 (-6)		
SiS	3.5 (-6)	< 1.4 (-7)	< 5.0 (-7)		
SO <sub>2</sub>	3.0 (-7)	1.3 (-5)			
H <sub>2</sub> S	1.3 (-5)	7.5 (-7)			
H <sub>2</sub> CO	5.0 (-7)		4.0 (-8)		
CO	4.0 (-4)	2.8 (-4)			
HCO <sup>+</sup>	3.0 (-8)	8.4 (-8)			
OCS	9.0 (-10)	1.1 (-6)			
CN	2.3 (-7)	< 2.0 (-7)			
N <sub>2</sub> H <sup>+</sup>	4.9 (-11)	< 1.6 (-8)			
HCS <sup>+</sup>	2.0 (-8)	< 1.5 (-7)			
NH <sub>3</sub>	1.0 (-5)	1.0 (-6)			
CH <sub>3</sub> OH	3.5 (-8)			< 4.1 (-8)	
C <sub>2</sub> H	1.9 (-7)			< 1.8 (-7)	

**Table 5.** A comparison of the peak calculated fractional abundances in the model for TX Cam with the observations of this region. The references for the observations are (1) Bujarrabal et al (1994); (2) Olofsson et al (1991); (3) Lindqvist et al (1988); (4) Charnley & Latter (1996).

Species	Model	Observations			
		1	2	3	4
HCN	2.7 (-7)	2.2 (-6)	1.0 (-6)	1.4 (-6)	
HNC	1.4 (-8)	1.3 (-7)			
SiS	3.5 (-6)	1.5 (-6)		1.2 (-6)	
CS	3.3 (-7)	4.6 (-7)	1.0 (-6)	5.0 (-7)	
SiO	3.2 (-5)	3.0 (-5)			
SO	7.8 (-7)	1.8 (-6)			
CN	2.6 (-7)		2.0 (-7)	< 5.0 (-6)	
NO	4.4 (-6)		< 8.0 (-5)		
HCO <sup>+</sup>	6.6 (-8)		< 4.0 (-7)		
CH <sub>3</sub> OH	1.4 (-8)			< 4.3 (-7)	
C <sub>2</sub> H	7.7 (-7)			< 8.7 (-7)	



and destroyed by photons.

PO is formed by the reaction of oxygen atoms with either PH or PH<sub>2</sub>. Destruction is by photodissociation.

Carbon-phosphorus molecules are not formed because of the lack of formation routes involving CH<sub>3</sub> and CH<sub>3</sub><sup>+</sup>.

**Table 6.** The peak fractional abundances calculated in the model of IK Tau compared with the observations. The references are (1) Bujarrabal et al (1985); (2) Omont et al (1993); (3) Lindqvist et al (1988); (4) Charnley & Latter (1996)

Species	Model	Observations			
		1	2	3	4
HCN	1.4 (-7)	9.8 (-7)		6.0 (-7)	
HNC	2.0 (-8)	5.2 (-8)		< 2.0 (-7)	
SiS	3.5 (-6)	4.4 (-7)		< 7.0 (-7)	
CS	2.9 (-7)	1.0 (-7)		3.0 (-7)	
SiO	3.2 (-5)	1.7 (-5)	3.0 (-6)		
SO	9.1 (-7)	2.6 (-6)	1.8 (-6)		
SO <sub>2</sub>	2.2 (-7)		4.1 (-6)		
H <sub>2</sub> S	1.3 (-5)				
HCO <sup>+</sup>	3.9 (-8)		-		
CH <sub>3</sub> OH	4.5 (-8)				1.2 (-7)
C <sub>2</sub> H	2.3 (-7)				-

#### 4. A comparison with observations

Observations are available for 3 of our sources, the exception being RDr.

OH231.8+4.2 is an unusual source with a strong bipolar outflow in which there is likely to be shocks which will affect the chemistry. We have not attempted to model this but instead have concentrated on the CSE itself. In view of this, the model gives surprisingly good agreement for a number of molecules: CS, SO, HCO<sup>+</sup>, CO, CN, N<sub>2</sub>H<sup>+</sup> and HCS<sup>+</sup> (see Table 4). Only an upper limit is available for the last 3 of these molecules. The available data for HCN show a considerable degree of variation with a fractional abundance of  $\sim 3\text{--}4 \times 10^{-7}$  being found by Morris et al (1987) and Lindqvist et al (1992), and a value about 10 times higher determined by Bujarrabal et al (1994). Our model agrees with the lower value. HNC is a factor of 10 lower than the observations but the ratio of HCN/HNC agrees with that found by Bujarrabal et al.

SiO, SiS, CO, H<sub>2</sub>S and NH<sub>3</sub> have been assumed to be parent molecules. Any differences between the model and the observations for these species therefore reflects a problem with the input abundances. CO is in agreement with the observations but the others show some discrepancies. SiO, SiS and NH<sub>3</sub> are calculated to have abundances considerably larger than observed. H<sub>2</sub>S is in agreement with the observations of Omont et al (1993) (who find that  $f(\text{H}_2\text{S})$  may be as large as  $10^{-5}$  at  $R = 10^{16}$  cm) but is considerably larger than the abundance found by Morris et al (1987). As stated in the introduction no attempt has been made here to customize the input abundances for a particular source and it may be that for OH231.8+4.2 the abundances of silicon and nitrogen are lower than we have assumed due to a greater incorporation into dust grains.

The calculated abundance of OCS shows poor agreement with the observations. SO<sub>2</sub> is also underabundant in our models. The observed abundance for SO<sub>2</sub> of  $1.3 \times 10^{-5}$  means that it contains 80 % of the solar abundance of sulphur. It is possible that the SO<sub>2</sub> arises in a different part of the source than the other

sulphur molecules and is formed for example in the shocks in the bipolar outflow (Jackson & Nguyen-Q-Rieu 1988).

Recently Charnley & Latter (1996) have undertaken a search for CH<sub>3</sub>OH and C<sub>2</sub>H in CSEs in order to place limits on the amount of CH<sub>4</sub> which could be present in the envelope as a parent molecule. Neither of these molecules were detected in any of the sources observed but upper limits were obtained. Our model results are in accord with their upper limits in contrast to the model of Charnley & Latter which predicted an overabundance of these two molecules. In the next section we consider the differences between the two models and the implications of these observations for the chemistry of CSEs.

Of the 11 molecules for which data is available, our model can reproduce the peak fractional abundances of all but 3 of them in TX Cam. HCN and HNC are again too low but their ratio is correct. For NO, HCO<sup>+</sup>, CH<sub>3</sub>OH and C<sub>2</sub>H upper limits only are available with which our model is consistent. Bujarrabal et al (1994) find a value for SO which is 3 times higher than our model and other observations by Sahai & Wannier (1992) put the fractional abundance even higher at  $3.2 - 6.5 \times 10^{-6}$ .

IK Tau is the only source for which the calculated abundance of HNC agrees with the observations. However in this case the abundance of HCN is too low. CS and SO are also in good agreement with SiO fitting the observations of Bujarrabal et al (1994) but not those of Omont et al (1993). SiS is calculated to be about 10 times higher than observed and this may argue for its abundance at the start of the model to be reduced. The SO<sub>2</sub> abundance is too low to account for the observations.

We conclude this section with a listing of the calculated column densities for a variety of species (Table 7).

#### 4.1. Is the presence of CH<sub>4</sub> as a parent molecule compatible with the observations?

Charnley & Latter (1996) found upper limits to the abundance of CH<sub>3</sub>OH and C<sub>2</sub>H in several CSEs and modelled 3 of them including TX Cam and IK Tau. Their calculations produced abundances which are too high (in some cases as much as an order of magnitude too high) to fit the observations. In addition they cannot reproduce the observed CS/SO ratio which is always less than 1. Our model can fit both these observational facts.

The models differ in that they use different versions of the UMIST ratefile but apart from that appear to be essentially the same. The updates in the rate coefficients in the ratefile used in our calculations are not sufficient to account for the variations in the results and we have no explanation for this. Here we present the differences between our models but without any attempt to account for them.

We have found a difference in the chemistry of CS and SO. In the model of Charnley & Latter CS and SO are closely linked, with CS forming from



(75)

**Table 7.** The calculated column densities in each model for a variety of species.

Species	OH231.8+4.2	IK Tau	TX Cam	R Dor
N <sub>2</sub> H <sup>+</sup>	6.4 (10)	5.7 (9)	6.6 (9)	1.1 (9)
NH <sub>3</sub>	1.8 (17)	1.1 (16)	8.0 (15)	2.0 (14)
HCN	8.8 (13)	2.4 (13)	4.5 (13)	1.2 (13)
HNC	1.5 (13)	3.4 (12)	2.4 (12)	7.1 (11)
CN	1.7 (14)	3.9 (13)	3.1 (13)	1.0 (13)
H <sub>2</sub> CN	1.9 (13)	6.2 (12)	8.4 (12)	2.1 (9)
CH <sub>3</sub> CN	9.9 (11)	3.2 (11)	7.9 (11)	1.6 (11)
SiN	3.8 (13)	1.2 (13)	1.2 (13)	3.1 (12)
SiS	6.8 (16)	4.8 (15)	3.6 (15)	2.3 (14)
SiO	6.1 (17)	4.5 (16)	3.4 (16)	2.7 (15)
SiO <sub>2</sub>	1.1 (15)	3.9 (14)	4.6 (14)	4.2 (13)
HCSi	1.4 (14)	5.0 (13)	7.3 (13)	2.5 (13)
SiCH <sub>2</sub>	6.5 (12)	2.0 (12)	3.5 (12)	6.4 (11)
CS	2.1 (14)	4.8 (13)	5.6 (13)	1.3 (13)
H <sub>2</sub> CS	8.0 (12)	2.1 (12)	3.9 (12)	5.2 (11)
SO	9.4 (14)	2.6 (14)	2.0 (14)	3.1 (13)
SO <sub>2</sub>	2.1 (14)	4.6 (13)	2.8 (13)	3.4 (12)
H <sub>2</sub> S	2.3 (17)	1.3 (16)	8.8 (15)	1.2 (14)
CO	7.9 (18)	6.2 (17)	4.8 (17)	4.6 (16)
CO <sup>+</sup>	1.2 (10)	6.0 (9)	3.9 (9)	1.2 (9)
CO <sub>2</sub>	3.0 (14)	9.4 (13)	6.4 (13)	7.0 (12)
HCO <sup>+</sup>	2.5 (13)	6.1 (12)	7.4 (12)	2.6 (12)
H <sub>2</sub> CO	4.8 (14)	1.4 (14)	2.2 (14)	4.0 (13)
OCS	6.2 (11)	1.9 (11)	5.5 (11)	8.6 (10)
C <sub>2</sub> H	1.9 (14)	5.1 (13)	1.5 (14)	3.0 (13)
C <sub>2</sub> H <sub>2</sub>	1.9 (13)	9.4 (12)	3.6 (13)	3.7 (12)
C <sub>2</sub> H <sub>3</sub>	4.9 (12)	2.3 (12)	3.8 (12)	6.8 (11)
C <sub>2</sub> H <sub>4</sub>	1.7 (13)	1.3 (13)	2.4 (13)	1.2 (12)
CH <sub>3</sub> <sup>+</sup>	6.7 (13)	2.6 (13)	6.6 (13)	1.7 (13)
CH <sub>3</sub>	2.0 (15)	7.3 (14)	5.9 (14)	1.1 (14)
CH <sub>4</sub>	5.6 (17)	3.5 (16)	2.5 (16)	6.4 (14)
CH <sub>3</sub> OH	2.7 (13)	1.2 (13)	3.6 (12)	5.3 (11)
CH <sub>2</sub> CO	1.2 (12)	2.8 (11)	2.7 (11)	5.1 (10)
H <sub>3</sub> O <sup>+</sup>	3.1 (13)	1.8 (13)	2.4 (13)	3.3 (12)
H <sub>2</sub> O	5.6 (18)	3.7 (17)	2.8 (17)	1.2 (16)
OH	1.2 (17)	3.5 (16)	2.7 (16)	6.6 (15)

In our model this reaction does make a contribution but it is not the principal formation route for CS. Instead CS forms from the reaction of HCS<sup>+</sup> with electrons



This is in agreement with Nejad & Millar (1988). However, in their model HCS<sup>+</sup> forms from



Charnley & Latter pointed out that H<sub>2</sub>S and C<sup>+</sup> exist in spatially distinct regions and therefore this reaction is unlikely to produce sufficient HCS<sup>+</sup> to account for the abundance of CS. In our model we find that HCS<sup>+</sup> forms from



thereby eliminating the problem.

In conclusion, we find that the presence of CH<sub>4</sub> as a parent molecule is not inconsistent with a CS/SO ratio of less than one and the upper limits of CH<sub>3</sub>OH and C<sub>2</sub>H.

## 5. Conclusions

Overall our model produces results which are in good agreement with the observations. In particular we have found that the presence of CH<sub>4</sub> as a parent molecule can account for the observations of carbon-bearing molecules in oxygen-rich CSEs and is not inconsistent with any of the available data. The chemistry of HCN and HNC is still not entirely clear with the calculated abundances of these molecules varying by up to an order of magnitude from the observed value.

The results for OH231.8+4.2 are the most unexpected as this is a complicated source and we have modelled just one part of it. Even so our model is very successful. An exception is SO<sub>2</sub> whose calculated abundance is too low in all the sources with the discrepancy being most marked for OH231.8+4.2. This may indicate that some of the emission for this molecule arises in the outflow region rather than the circumstellar envelope itself. The results for other sulphur molecules agree with the observations and in particular we can account for the observed ratio of CS/SO which is always < 1.

Phosphorus-carbon species are not formed in appreciable quantities because of the lack of formation reactions involving either CH<sub>3</sub> or its ion.

## References

- Bujarrabal V., Fuente A., Omont A., 1994, A&A 285 247  
 Charnley S. B., Tielens A. G. G. M., Kress M. E., 1995, MNRAS 274 L53  
 Charnley, S. B., Latter W. B., 1996, MNRAS submitted  
 Charnley S. B., Millar T. J., 1994, MNRAS 270 570  
 Deguchi S., Goldsmith P. F., 1985, Nature 317 336  
 Jackson, J. M., Nguyen-Q-Rieu, 1988, ApJ, 335 L83  
 Jewell P. R., Snyder L. E., Schenework M. E., 1986, Nature 323 311  
 Lindqvist M., Olofsson H., Winnberg A., Nyman L.-Å., 1992, A&A 263 183  
 Lindqvist M., Nyman L.-Å., Olofsson H., Winnberg A., 1988, A&A 205 L15  
 Millar T. J., Farquhar P. R. A., Willacy K., 1997, A&A 121 139  
 Millar, T. J., Olofsson, H., 1993, MNRAS 262, L55  
 Morris M., Jura M., 1983, ApJ 264 546  
 Morris M., Guilloteau S., Lucas R., Omont A., 1987, ApJ 321 888  
 Nejad, L. A. M., Millar, T. J., 1988, MNRAS 230 79  
 Nercessian, E., Guilloteau, S., Omont, A., Benayoun, J. J., 1989, A&A 210 225  
 Olofsson H., Lindqvist M., Winnberg A., Nyman L.-Å., Nguyen-Q-Rieu, 1991, A&A 245 611  
 Olofsson H., Johansson L. E. B., Hjalmarsen Å., Nguyen-Quang-Rieu, 1982, A&A 107 128  
 Omont, A., Forveille, T., Guilloteau, S., Lucas, R., 1986, IAU Symposium 122, 511 eds Appenzeller, I., Jordan, C.,  
 Omont A., Lucas R., Morris M., Guilloteau S., 1993, A&A 267 490  
 Sahai, R., Wannier, P. G., 1992, ApJ 320 394  
 Tsuji T., 1973, A&A 23 411

This article was processed by the author using Springer-Verlag L<sup>A</sup>T<sub>E</sub>X A&A style file L-AA version 3.